

Non-equilibrium quantum phase transition via entanglement decoherence dynamics

Yu-Chen Lin,¹ Pei-Yun Yang,¹ and Wei-Min Zhang^{1,*}

*¹Department of Physics and Centre for Quantum Information Science,
National Cheng Kung University, Tainan 70101, Taiwan*

Abstract

We investigate the decoherence dynamics of continuous variable entanglement as the system-environment coupling strength varies from the weak-coupling to the strong-coupling regimes. Due to the existence of localized modes in the strong-coupling regime, the system cannot approach equilibrium with its environment, which induces a nonequilibrium quantum phase transition. We analytically solve the entanglement decoherence dynamics for an arbitrary spectral density. The nonequilibrium quantum phase transition is demonstrated as the system-environment coupling strength varies for all the Ohmic-type spectral densities. The 3-D entanglement quantum phase diagram is obtained.

*Electronic address: wzhang@mail.ncku.edu.tw

In quantum many-body systems, quantum phase transitions (QPTs) may occur at zero temperature as a parameter varies in the Hamiltonian of the system, induced purely by quantum fluctuations [1]. QPTs have been explored via entanglement [2–6], because entanglement is regarded as a key resource to detect QPTs, owing to the fact that the entanglement can exist without any classical correlations [7]. In previous investigations, QPTs are usually investigated in terms of entanglement for the many-body systems via the von Neumann entropy by dividing the system into various bipartites. In these investigations, significant changes of the entanglement as a parameter varies in the Hamiltonian of the system provide a deeper understanding about QPTs.

In order to experimentally explore QPTs, it is crucial how to manipulate the basic parameters in the Hamiltonian of the system, such as hopping energies and interaction coupling strengths, etc. through the external devices. Thus, these systems manifesting QPTs become naturally open systems [8–10]. In this article, we attempt to explore nonequilibrium QPTs by studying the entanglement decoherence dynamics in a prototype open quantum system of two entangled modes interacting with a general non-Markovian environment. We find that entanglement decoherence dynamics, induced by the interaction between the system and its environment, manifests a significant change as the system-environment coupling strength varies from the weak to the strong coupling regimes. Nonequilibrium quantum phase transition occurs due to the competition between quantum dissipation dynamics and localization. Thermal fluctuations can drive further the entanglement decoherence dynamics into a quantum critical regime and then into the thermal disordered regime. This could open a new venue for the experimental investigations of QPTs through the real-time entanglement decoherence dynamics.

Results

Real-time exact solution of entangled squeezed states. We consider a system with two entangled continuous variables, such as two entangled cavity fields, interacting to a common thermal environment, its dynamics is described by the Fano-Anderson Hamiltonian [11, 12],

$$\begin{aligned}
 H_{tot} = & \omega_1 a_1^\dagger a_1 + \omega_2 a_2^\dagger a_2 + \kappa(a_1^\dagger a_2 + a_2^\dagger a_1) \\
 & + \sum_k \omega_k b_k^\dagger b_k + \sum_{i=1,2,k} (g_{ik} a_i^\dagger b_k + g_{ik}^* b_k^\dagger a_i),
 \end{aligned} \tag{1}$$

where a_i and a_i^\dagger ($i=1,2$) are the annihilation and creation operators of the two continuous

variables with frequency ω_i , and κ is a real coupling constant between the two continuous variables, which can be tuned, for example, through a beam splitter on the two single-mode fields [13]. The environment Hamiltonian consists of an infinite number of bosonic modes, where b_k and b_k^\dagger are the annihilation and creation operators of the mode k with frequency ω_k . The interaction between the system and the environment is given by the last term in Eq. (1), and the parameter g_{ik} is the coupling amplitude between the continuous variable mode i and the environment mode k . The complexity of the problem is embedded in the spectral density, see Eq. (5) later, which characterizes the complicated energy structure of the environment plus the system-environment interaction.

In order to investigate the entanglement decoherence dynamics of the two continuous variables under the influence of a complicated environment, we take a decoupled initial state between the system and the environment [14]: $\rho_{tot}(0) = \rho_s(0) \otimes \rho_E(0)$. The initial state of the system is $\rho_s(0) = |\psi_s(0)\rangle\langle\psi_s(0)|$, where $|\psi_s(0)\rangle$ is an entangled state between the two continuous variables, and the environment is initially in thermal equilibrium $\rho_E(0) = \frac{1}{Z} \exp\{-\beta \sum_k \omega_k b_k^\dagger b_k\}$ at the initial inverse temperature $\beta = 1/k_B T$. After the initial time, the system and the environment both dynamically evolve into non-equilibrium states. To be specific, let $\rho_s(0)$ be a two-mode squeezed state [15],

$$|\psi_s(0)\rangle = S_{12}(r)|00\rangle, \quad (2)$$

where $S_{12}(r) = \exp\{ra_1a_2 - ra_1^\dagger a_2^\dagger\}$ is a two-mode squeezed operator, and r is the real squeezing parameter. This state has been experimentally realized in many different systems, first given by Heidmann *et al* [16], and has also been applied to quantum teleportation [17]. When the squeezing parameter becomes very large, the above state would approach to the ideal Einstein-Podolsky-Rosen (EPR) state [18].

Without loss of generality, we may consider the two continuous variables as two identical fields and interact homogeneously with the environment, namely, $\omega_1 = \omega_2 = \omega_0$ and $g_{ik} = g_k$. Then we can introduce the center-of-mass and the relative motional variables, respectively, given by $a_+^\dagger = (a_1^\dagger + a_2^\dagger)/\sqrt{2}$, and $a_-^\dagger = (a_1^\dagger - a_2^\dagger)/\sqrt{2}$, with the corresponding frequencies $\omega_\pm = \omega_0 \pm \kappa$. It is easy to check that only the center-of-mass variable a_+ is coupled with the environment, and the relative-motional variable decouples from the environment which forms a decoherence-free subspace [19]. If the two continuous variables are not identically coupled to the environment, no such decoherence-free subspace exists, and the decoherence dynamics

of the relative motion behaves similarly as that of the center-of-mass motion. In terms of the center-of-mass motion and the relative motion of the two continuous variables, we can rewrite the initial state (2) as a direct product of two entangled states, $|\psi_s(0)\rangle = |\psi_+(0)\rangle \otimes |\psi_-(0)\rangle$, where

$$|\psi_{\pm}(0)\rangle = \exp\left[\pm \frac{r}{2}(a_{\pm})^2 \mp \frac{r}{2}(a_{\pm}^{\dagger})^2\right]|0\rangle. \quad (3)$$

Because the relative motion a_- is decoupled from the environment, the entanglement between the two continuous variables in $|\psi_-(0)\rangle$ is decoherence-free. Therefore, the entanglement decoherence only happens to the center-of-mass motion.

More specifically, entanglement decoherence dynamics is fully determined by the spectral density of the environment, which is defined by $J_{ij}(\omega) = \sum_k g_{ik}g_{jk}^* \delta(\omega - \omega_k)$. When the two continuous variables identically couple to the common environment: $g_{ik} = g_k$, we have $J_{ii}(\omega) = |J_{12}(\omega)|$. In the center-of-mass frame, the spectral density is simply reduced to

$$\mathbf{J}(\omega) = \begin{pmatrix} J_{++}(\omega) & J_{+-}(\omega) \\ J_{-+}(\omega) & J_{--}(\omega) \end{pmatrix} = \begin{pmatrix} 2J(\omega) & 0 \\ 0 & 0 \end{pmatrix}, \quad (4)$$

it shows that $J_{--}(\omega) = 0$. This indicates that the environment synchronizes quantum as well as thermal fluctuations at the two identical parties, so that the relative motion experiences no fluctuation. Consequently, the corresponding entanglement contribution remains unchanged as the initial value for the relative motion (i.e. decoherence-free), as we will see more discussion later. The decoherence dynamics of the center-of-motion part is then fully controlled by the spectral component $J_{++}(\omega) = 2J(\omega)$. In the following, we consider the Ohmic-type spectral density [14] which can simulate a large class of thermal bath,

$$J(\omega) = \sum_k |g_k|^2 \delta(\omega - \omega_k) = \eta \omega \left(\frac{\omega}{\omega_c}\right)^{s-1} \exp\left(-\frac{\omega}{\omega_c}\right), \quad (5)$$

where η is a dimensionless coupling strength between the system and the environment, and ω_c is the cutoff of the environment spectrum. The parameter s classifies the environment as sub-Ohmic ($s < 1$), Ohmic ($s = 1$), or super-Ohmic ($s > 1$). Although we focus on such a general environmental structure, the results are valid to other spectral densities (other environmental structures) that do not be described by Eq. (5).

The real-time dynamics of the initial state (2) can be solved directly from the reduced density matrix: $\rho_s(t) = \text{Tr}_E[\mathcal{U}(t, 0)\rho_{tot}(0)\mathcal{U}^{\dagger}(t, 0)]$, where $\mathcal{U}(t, 0) = \exp\{-iH_{tot}t\}$ is the unitary

evolution operator of the total system (the two entangled fields coupled their environment). The general solution is given by

$$\rho_s(t) = \rho_+(t) \otimes \rho_-(t) \quad (6)$$

where $\rho_+(t)$ is the reduced density matrix of the center-of-mass motion, and the relative motion remains a pure state $\rho_-(t) = |\psi_-(t)\rangle\langle\psi_-(t)|$. The explicit analytical solution can be solved with the results

$$|\psi_-(t)\rangle = S[r_-(t)]|0\rangle, \quad (7)$$

$$\rho_+(t) = S[r_+(t)]\rho_{\text{th}}(t)S^\dagger[r_+(t)] \quad (8)$$

where $S[r_\pm(t)] = \exp\left[\frac{r_\pm^*(t)}{2}(a_\pm)^2 - \frac{r_\pm(t)}{2}(a_\pm^\dagger)^2\right]$ is the time-evolving squeezing operators of the center-of-mass motion and the relative motion of the two fields, and Eq. (8) is a time-evolving thermal-like squeezed state [20]. Explicitly, the squeezing parameters

$$r_-(t) = -re^{-i2\omega t}, \quad r_+(t) = |r_+(t)|e^{i\theta_+(t)} \quad (9)$$

with $|r_+(t)| = \frac{1}{4} \ln \frac{n_+(t)+|\sigma_+(t)|+1/2}{n_+(t)-|\sigma_+(t)|+1/2}$ and $\theta_+(t) = \arg[\sigma_+(t)]$. The nonequilibrium thermal-like state

$$\rho_{\text{th}}(t) = \sum_n \frac{[\bar{n}_+(t)]^n}{[1 + \bar{n}_+(t)]^{n+1}} |n\rangle_{++} \langle n|, \quad (10)$$

where $|n\rangle_+ = \frac{1}{\sqrt{n!}}(a_+^\dagger)^n|0\rangle$ is the Fock state of the center-of-mass variable, and the average particle number in this state, $\bar{n}_+(t) = \text{Tr}[a_+^\dagger a_+ \rho_{\text{th}}(t)]$, describes the nonequilibrium thermal fluctuations and satisfies the relation

$$\bar{n}_+(t) + 1/2 = \sqrt{[n_+(t) + 1/2]^2 - |\sigma_+(t)|^2}. \quad (11)$$

The factor 1/2 in the above equation is related to the zero-point energy fluctuation, and $n_+(t)$ and $\sigma_+(t)$ are respectively the photon intensity (the squeezed thermal fluctuation) and the two-photon correlation of the center-of-mass variable,

$$n_+(t) = \text{Tr}[a_+^\dagger a_+ \rho_+(t)] = |u_+^2(t, 0)| \sinh^2 r + v_+(t, t), \quad (12)$$

$$\sigma_+(t) = \text{Tr}[a_+ a_+ \rho_+(t)] = -u_+^2(t, 0) \cosh r \sinh r. \quad (13)$$

The functions $u_+(t, 0)$ and $v_+(t, t)$ are Schwinger-Keldysh's retarded and correlated (fluctuation) Green functions in nonequilibrium many-body systems [21–23] for the center-of-mass

variable, and they obey the Kadanoff-Baym equations [23] and the dissipation-fluctuation theorem [24], respectively,

$$\dot{u}_+(t, 0) + i\omega_+ u_+(t, 0) + \int_0^t d\tau g(t, \tau) u_+(\tau, 0) = 0, \quad (14)$$

$$v_+(t, t) = \int_0^t d\tau_1 \int_0^t d\tau_2 u_+(t, \tau_1) \tilde{g}(\tau_1, \tau_2) u_+^\dagger(t, \tau_2), \quad (15)$$

in which the integral kernels, $g(t, t') = 2 \int d\omega J(\omega) e^{-i\omega(t-t')}$ and $\tilde{g}(t, t') = 2 \int d\omega J(\omega) \bar{n}(\omega, T) e^{-i\omega(t-t')}$, are fully determined by the spectral density of the environment. Here, $\bar{n}(\omega, T) = 1/[e^{\beta\omega} - 1]$ is the initial particle distributions in the environment.

The above analytical solutions show explicitly that the squeezed parameter in the relative-motion state $\rho_-(t)$ only takes a simple oscillation and is therefore decoherence-free. This is because the environment which equally couples to the two identical fields synchronizes both quantum (dissipation) and thermal fluctuations at the two identical parties so that the relative motion experiences no fluctuation, as a consequence of $J_{--}(\omega) = 0$. On the other hand, all the environment-induced quantum (dissipation) and thermal fluctuations derive the center-of-mass motion part from an initial pure squeezed state into a thermal-like squeezed state $\rho_+(t)$, see Eq. (8) in which the squeezed operator $S[r_+(t)]$ acts on the nonequilibrium thermal-like state $\rho_{th}(t)$. The nonequilibrium thermal-like state $\rho_{th}(t)$, which is induced by the environment, is different from the usual equilibrium thermal state because the averaged particle number $\bar{n}_+(t)$ in $\rho_{th}(t)$ is not equal to the standard Bose-Einstein distribution $\bar{n}(\omega, T)$ at the given frequency ω and the given equilibrium temperature T . Geometrically, $\rho_{th}(t)$ is also symmetrically distributed in terms of the quadrature components of the center-of-mass variable with $\Delta X_+(t) = \Delta P_+(t) = \sqrt{\bar{n}_+(t) + 1/2}$, where $\bar{n}_+(t)$ and $1/2$ characterize the thermal and vacuum fluctuations, respectively. The squeezed parameter $r_+(t)$ is governed by both the quantum fluctuation $\sigma_+(t)$ and the thermal fluctuations embedded in the intensity $n_+(t)$ of the center-of-mass variable. The relation given by Eq. (11), $n_+(t) + 1/2 = \sqrt{[\bar{n}_+(t) + 1/2]^2 + |\sigma_+(t)|^2}$ describes how the thermal-like state $\rho_{th}(t)$, is squeezed by the quantum fluctuation $\sigma_+(t)$ through the squeezing operator $S(r_+(t))$: $\Delta X_+(t) \rightarrow \sqrt{\bar{n}_+(t) + 1/2} e^{-|r_+(t)|}$ and $\Delta P_+(t) \rightarrow \sqrt{\bar{n}_+(t) + 1/2} e^{|r_+(t)|}$. If $\sigma_+(t) \rightarrow 0$, we have $r_+(t) \rightarrow 0$ and $S(r_+(t)) \rightarrow 1$. Then the center-of-mass motion approaches to a thermal state due to thermal fluctuations of the environment only.

Nonequilibrium entanglement decoherence dynamics.

The above analytical solutions show that the entanglement decoherence dynamics can be fully determined from the solution of Eq. (14) which provides the general quantum dissipation dynamics in open quantum systems [24],

$$u_+(t, 0) = \sum_j Z_j e^{-i\bar{\omega}_j t} + 2 \int \frac{d\omega J(\omega) e^{-i\omega t}}{(\omega - \omega_+ - \Delta(\omega))^2 + 4\pi^2 J^2(\omega)}, \quad (16)$$

where the first term is contributed by the localized modes in the Fano-Anderson model [24, 25], with the frequencies $\bar{\omega}_j$ which are determined by the zeros of the function $z(\omega) \equiv \omega_+ - \omega + \Delta(\omega)$, and the amplitude $Z_j = 1/(1 - \Sigma'(\bar{\omega}_j))$ is the corresponding pole residue. Here $\Sigma(\omega) = 2 \int d\omega' \frac{J(\omega')}{\omega - \omega'}$ is the self-energy, and $\Delta(\omega) = 2\mathcal{P} \int d\omega' \frac{J(\omega')}{\omega - \omega'}$ denotes its principal value. This localized mode contributes a dissipationless dynamics. The second term in Eq. (16) always decays, which leads to the quantum dissipation (damping) dynamics in open systems. For the spectral density of Eq. (5), the localized mode occurs only when the dimensionless system-environment coupling strength is greater than the critical coupling strength $\eta_c(s)$ for a given environment characterized by s ,

$$\eta > \eta_c(s) \equiv \frac{\omega_+}{2\omega_c \Gamma(s)}, \quad (17)$$

where $\Gamma(s) = \int_0^\infty x^{s-1} e^{-x} dx$ is the gamma function. On the other hand, the environment-induced fluctuations is characterized by $v_+(t, t)$, which is determined by Eq. (15) as a result of the generalized nonequilibrium fluctuation-dissipation theorem in the time-domain.

Now we can see that the center-of-mass state $\rho_+(t)$ contains various decoherence dynamics. For a given spectral density (fixed s), the state $\rho_+(t)$ in the strong-coupling regime ($\eta > \eta_c(s)$) undergoes a partial decoherence process and then approach to a nonequilibrium state, due to the existence of the localized mode [25–30]. This property becomes obvious by looking at the initial state dependence, the squeezed parameter r -dependence in the time-dependent coefficients in Eqs. (12-13). This initial-state dependence is a manifestation of the strong non-Markovian memory effect, induced by the localized mode in the strong coupling, see Eq. (16). Thus, when $\eta > \eta_c(s)$, $\rho_+(t)$ becomes a nonequilibrium entanglement state that always depends on the initial state, even in the steady-state limit $t \rightarrow \infty$. Only in the weak-coupling regime ($\eta < \eta_c(s)$), the localized mode cannot be formed, and the Green function $u_+(t, 0) \rightarrow 0$ as $t \rightarrow \infty$ so that $\sigma_+(t) \rightarrow 0$. Then the time-dependent squeezing parameter $r_+(t) \rightarrow 0$. As a result, the state $\rho_+(t)$ will approach to thermal equilibrium state,

$$\rho_+(t \rightarrow \infty) = \rho_{\text{th}}(t \rightarrow \infty) \quad (18)$$

with the average particle number (thermal fluctuation) $\bar{n}_+ = n_+ = v_+(t \rightarrow \infty)$. This state is independent of the initial squeezed state, and also contains no any entanglement. In other words, when $\eta < \eta_c(s)$, the system reaches equilibrium with its environment, and the entanglement of the center-of-mass state $\rho_+(t)$ is completely decohered away.

To be explicit, we should quantitatively study the entanglement decoherence dynamics by quantifying the entanglement between the two continuous variables in the two-mode entangled state, using the logarithmic negativity [31]. The logarithmic negativity has been widely used in the literature, based on the Peres-Horodecki positive partial transpose (PPT) criterion [32] as a necessary and sufficient condition for the separability of bipartite Gaussian states. The entanglement degree of a bipartite Gaussian state is given by [31]:

$$E_N = \max\{0, -\log_2(2\tilde{\lambda}_2)\}. \quad (19)$$

where $\tilde{\lambda}_2$ is the smaller one of the two symplectic eigenvalues of the covariant matrix. On the other hand, if the entangled state is a direct product of two entangled states, the total entanglement is also the sum of the logarithmic negativities from each state [31]. Meanwhile, we also find that for the case of the direct product state, like Eq. (6), in which one state undergoes a decoherence process and the other state is decoherence-free, one must calculate the entanglement from each state separately in the product and then add them together to get the correct total entanglement. If one uses the logarithmic negativity to calculate the entanglement directly from the original state, then the decoherence dynamics in one state will artificially decohere away the entanglement in the decoherence-free state. This will lead to a unphysical solution. Thus, the total entanglement between the two original continuous variables in $\rho_s(t)$ is given by

$$E_N = E_N(\rho_+(t)) + E_N(\rho_-(t)). \quad (20)$$

It is not difficult to find that for the initial state (2), the entanglement $E_N(\rho_+(0)) = E_N(\rho_-(0)) = r/\ln 2$, namely, the initial total entanglement is equally distributed between the relative-motion state $|\psi_-(0)\rangle$ and the center-of-mass state $|\psi_+(0)\rangle$.

The real-time dynamics of the entanglement for each part in Eq. (20) can be solved analytically. For the relative-motion state $\rho_-(t)$, because of its decoupling from the thermal reservoir, its entanglement remains *unchanged*, $E_N(\rho_-(t)) = r/\ln 2$. On the other hand, for the center-of-mass motion state $\rho_+(t)$, the time evolution of the entanglement can be

determined through Eq. (19). It is not difficult to find the smaller symplectic eigenvalue $\tilde{\lambda}_2(t)$ of the covariant matrix with respect to the two original continuous variables for $\rho_+(t)$,

$$\tilde{\lambda}_2(t) = \frac{1}{\sqrt{2}} \sqrt{n_+(t) - |\sigma_+(t)| + 1/2}. \quad (21)$$

Then $E_N(\rho_+(t))$ can be computed from the nonequilibrium retarded and correlated Green functions $u_+(t, 0)$ and $v_+(t, t)$ through Eqs. (12) and (13). The retarded Green function $u_+(t, 0)$ describes the dissipation dynamics, which is independent of the initial temperature of the environment, and manifests pure quantum correlations between the system and the environment [24]. The correlation Green function $v_+(t, t)$, the generalized nonequilibrium fluctuation-dissipation theorem, depends explicitly on the initial environment temperature, it describes the thermal fluctuations and the thermal-fluctuation-induced quantum fluctuations. The dynamics of the total entanglement of the two continuous variables with the initial state (2) is given by $E_N = E_N(\rho_+(t)) + r/\ln 2$.

We first consider the weak-coupling regime $\eta < \eta_c(s)$ at zero temperature, the function $u_+(t, t_0)$ will decay to zero for $t \rightarrow \infty$. Meanwhile, the correlation function $v_+(t, t) = 0$ because $\bar{n}(\omega, T) = 0$ at zero temperature. Thus the time-dependent functions in Eqs. (12-13) lead to $\sigma_+(t) = 0$ and $n_+(t) = 0$ as $t \rightarrow \infty$. As a result, Eq. (21) is reduce to $\tilde{\lambda}_2(t \rightarrow \infty) = \frac{1}{2}$ so that $E_N(\rho_+(t \rightarrow \infty)) = 0$. Then the steady-state total entanglement $E_N = E_N(\rho_-(t \rightarrow \infty)) = r/\ln 2$. This reproduces the result at zero temperature in the weak-coupling regime we obtained previously [33]. If the environment is initially at a finite temperature, because $u_+(t \rightarrow \infty, 0) \rightarrow 0$ is always true for $\eta < \eta_c(s)$, we have $n_+(t) \rightarrow v_+(t, t)$ and $\sigma_+(t) \rightarrow 0$ so that

$$-\log_2(2\tilde{\lambda}_2) = -\frac{1}{2\ln 2} \ln(1 + 2v_+(t, t)). \quad (22)$$

Also because $v_+(t, t) > 0$ for any finite temperature, Eq. (22) gives always a negative value. According to the criterion (19), again the entanglement of $\rho_+(t \rightarrow \infty)$ must go to zero. Indeed, Eq. (22) shows that thermal fluctuations speed up the entanglement decoherence. The steady-state entanglement $E_N(\rho_+(t \rightarrow \infty))$ remains zero in the weak-coupling regime ($\eta < \eta_c(s)$) for any initial environment temperature, and the steady-state total entanglement always equals to $E_N(\rho_-(t)) = r/\ln 2$.

Actually, the entanglement dynamics of Eq. (2) in the weak-coupling regime at finite temperature was previously studied in Ref. [34] where it shows that the decoherence lets the total entanglement be less than one half of the initial total entanglement due to the

thermal effect, see explicitly Fig. 8(b) in Ref. [34]. This is obviously a wrong result because the relative motion state $\rho_-(t)$ decouples from the environment such that the entanglement contained in $\rho_-(t)$ is decoherence-free. Thus, physically the steady-state total entanglement can never be less than $r/\ln 2$, as we shown above. The mistake made in Ref. [34] comes from an improper calculation of the entanglement when the entangled state is a direct product of two states. The improper calculation in Ref. [34] lets the entanglement decoherence dynamics of the center-of-mass motion artificially decohere the entanglement in the relative motion state, while the later is however decoherence-free. This leads to the wrong result of the steady-state total entanglement being less than $r/\ln 2$, as given in Ref. [34].

On the other hand, in the strong-coupling regime ($\eta > \eta_c(s)$), the propagating function $u_+(t, t_0)$ will not decay to zero in the steady-state limit, due to the existence of localized states [24, 25]. Thus the state $\rho_+(t)$ Eq. (8) cannot approach to a thermal equilibrium state because it maintains the initial-state dependence at $t \rightarrow \infty$, see Eqs. (12-13). Correspondingly, the entanglement dynamics undergoes a quantum phase transition as the system-environment coupling varying from the weak-coupling regime to the strong-coupling regime.

Nonequilibrium quantum phase transition. Now, we shall numerically analyze the entanglement dynamics for different spectral densities to demonstrate the quantum phase transition discussed above. Taking the sub-Ohmic reservoir ($s = 0.5$) as an example, we present the real-time dynamics of the entanglement in Fig. 1. As it shows, in the weak-coupling regime $\eta < \eta_c(s) = 0.141$ for $s = 0.5$, the entanglement of the center-of-mass motion is gradually decohered away. This is indeed true for all the three different Ohmic-type spectra given by Eq. (5). However, in the strong-coupling regime $\eta > \eta_c(s)$, the entanglement can be partially preserved, even in the long-time limit, due to the existence of the localized state which induces the long-time non-Markovian memory effect. This provides the real-time dynamics of the nonequilibrium quantum phase transition through entanglement decoherence as the system-environment coupling strength varies.

To understand the origin of the quantum phase transition, we present the quantum dissipation and fluctuations, described by the steady-state retarded Green function $u_+(t \rightarrow \infty, 0)$ and correlation Green function $v_+(t, t \rightarrow \infty)$, in Fig. 2. It shows that in the weak-coupling regime ($\eta < \eta_c(s)$), the amplitude of the retarded Green function $|u_+(t \rightarrow \infty, 0)|$ decays to zero, see the empty area in Fig. 2 (a). In the strong-coupling regime ($\eta > \eta_c(s)$), the

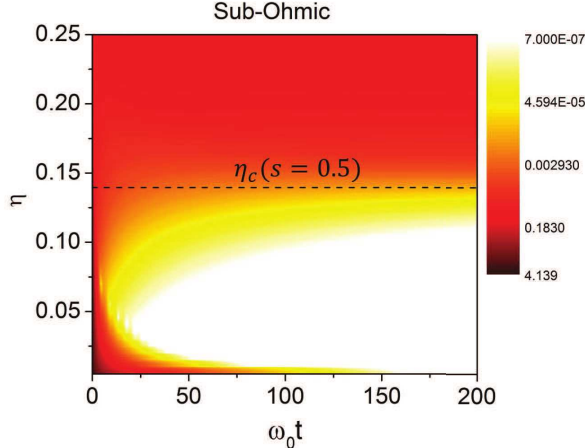


FIG. 1: **Real-time entanglement dynamics.** The contour plot of the entanglement $E_N(\rho_+(t))$ (in log scale) as a function of the time and the system-environment coupling strength η at zero initial environment temperature for sub-Ohmic spectral density. The other parameters are taken as $\omega_c = 3\omega_0$, $\kappa = 0.5\omega_0$ and $r = 3$.

localized mode occurs, then the amplitude of $u_+(t \rightarrow \infty, 0)$ maintains a nonzero value, given by the color area in Fig. 2 (a). This demonstrates clearly a quantum phase transition from dissipation dynamics to localization dynamics when the system-environment coupling passes through the critical coupling $\eta_c(s)$ for various spectral densities (different s). This phase transition is the first-order phase transition and is purely induced by quantum fluctuations. On the other hand, the corresponding steady-state fluctuation Green function $v_+(t, t \rightarrow \infty)$ presented in Fig. 2 (b) shows a huge amount of thermal fluctuations near the quantum critical transition line $\eta_c(s)$ (the dash line). When the coupling strength goes away from the critical regime around $\eta_c(s)$, the fluctuations decrease rapidly. This manifests the quantum criticality as a result of the competition between quantum fluctuations and thermal fluctuations.

With the above quantum criticality extracted from the fluctuation Green function $v_+(t, t)$, an entanglement phase diagram, in terms of the entanglement $E_N(\rho_+(t \rightarrow \infty))$ as a function of the system-environment coupling η , the spectral parameter s and the initial environment temperature T , is presented in Fig. 3. As we see, at zero temperature, the $\eta - s$ plane is separated into the quantum disordered ($\eta < \eta_c(s)$) and quantum ordered ($\eta > \eta_c(s)$) phases. When the initial environment temperature is nonzero, the competition between quantum fluctuations and thermal fluctuations shows up. As a result, the entanglement

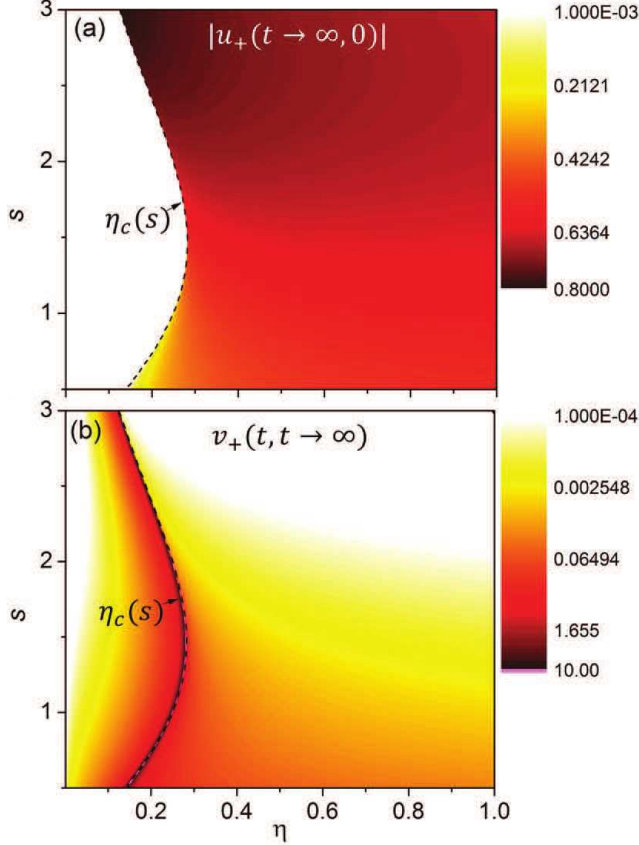


FIG. 2: **Localization and fluctuation dynamics.** (a) The localization given by the retarded Green function $|u_+(t \rightarrow \infty, 0)|$, and (b) the fluctuation in terms of the correlated Green function $v_+(t, t \rightarrow \infty)$ (in log scale) as a function of the coupling strength η and the spectral parameter s . The other parameters are taken as the same as in Fig. 1 but the initial environment temperature $T = 0.1\omega_0$.

protected by the localization in the strong-coupling regime can be gradually decohered away by thermal fluctuations, and the thermal disordered phase with $E_N(\rho_+(t \rightarrow \infty)) = 0$ is formed for $\eta > \eta_c(s)$ and $T > T_c(s, \eta)$, where $T_c(s, \eta)$ is a critical surface separating the quantum ordered phase and the thermal disordered phase, as shown in Fig. 3. Owing to the strong thermal fluctuation and small localized mode amplitude for the small value s , the thermal disordered phase starts to show up from the sub-Ohmic reservoir. Increasing the initial environment temperature will enhance thermal fluctuations such that the domain of the thermal disordered phase is enlarged, extending to the Ohmic and then super-Ohmic reservoir. It also shows that the transition from the quantum entangled phase to the thermal disordered phase is a continuous phase transition.

Discussions.

In this work, we find that entanglement decoherence, due to the environment-induced dissipation, localization and fluctuation dynamics, forms three different types of phases as the system-environment coupling strength η , the spectral parameter s and the initial environment temperature T vary: the dissipation-induced disentangled phase (phase I) in the weak-coupling regime $\eta < \eta_c(s)$ for arbitrary initial environment temperature; the quantum entangled phase (phase II, the colored part in Fig. 3) protected by the localized state in the strong-coupling regime $\eta > \eta_c(s)$ with $T < T_c(s, \eta)$, and the thermal disordered phase (phase III) as the result of thermal fluctuations dominating in the regime $\eta > \eta_c(s)$ and $T > T_c(s, \eta)$. The transition from phase I to phase II is the first-order quantum phase transition (corresponding to the transition of dissipation dynamics to localization dynamics [28, 29]), while transition from phase II to phase III is a continuous phase transition. The results presented in this article can be applied to other open systems [24]. This provides a general procedure to explore nonequilibrium quantum phase transition through the experimental measurement of real-time entanglement decoherence dynamics in many-body systems.

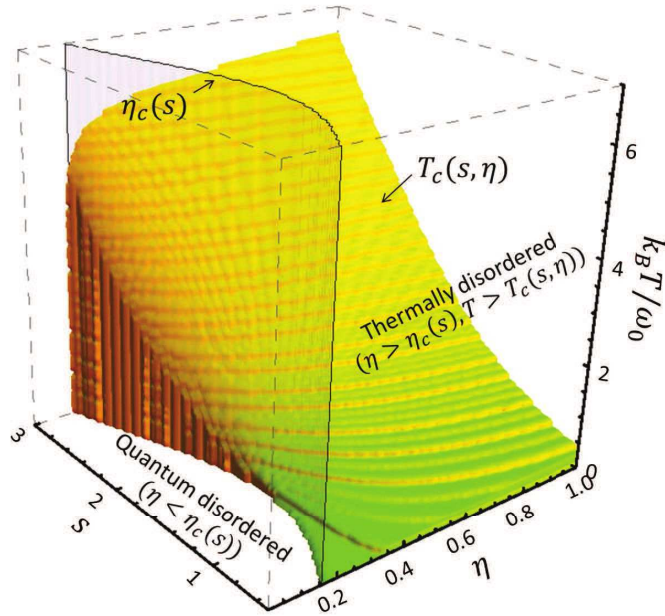


FIG. 3: **The 3-D phase diagram.** A contour plot of entanglement degree $E_N(\rho_+(t \rightarrow \infty))$ in 3-D space of the coupling strength η , the spectral parameter s and the initial reservoir temperature T . The other parameters are taken as the same as in Fig. 1.

-
- [1] Sachdev, S. *Quantum Phase Transitions*, 2nd Ed. (Cambridge University Press, 2011).
- [2] Osterloh, A., Amico, L., Falci, G. & Fazio, R. Scaling of entanglement close to a quantum phase transition. *Nature* **416**, 608-610, doi: 10.1038/416608a (2002).
- [3] Osborne, T. J. & Nielsen, M. A. Entanglement in a simple quantum phase transition. *Phys. Rev. A* **66**, 032110, doi: 10.1103/PhysRevA.66.032110 (2002).
- [4] Vidal, G., Latorre, J. I., Rico, E. & Kitaev, A. Entanglement in Quantum Critical Phenomena. *Phys. Rev. Lett.* **90**, 227902, doi: 10.1103/PhysRevLett.90.227902 (2003).
- [5] Gu, S. J., Deng, S. S., Li, Y. Q. & Lin, H. Q. Entanglement and Quantum Phase Transition in the Extended Hubbard Model. *Phys. Rev. Lett.* **93**, 086402, doi: 10.1103/PhysRevLett.93.086402 (2004).
- [6] Wu, L.-A., Sarandy, M. S. & Lidar, D. A. Quantum Phase Transitions and Bipartite Entanglement. *Phys. Rev. Lett.* **93**, 250404, doi: 10.1103/PhysRevLett.93.250404 (2004).
- [7] Kaszlikowski, D., Sen(De), A., Sen, U., Vedral, V. & Winter, A. Quantum Correlation without Classical Correlations. *Phys. Rev. Lett.* **101**, 070502, doi: 10.1103/PhysRevLett.101.070502 (2008).
- [8] Mitra, A., Takei, S., Kim, Y. B. & Millis, A. J. Nonequilibrium quantum criticality in open electronic systems. *Phys. Rev. Lett.* **97**, 236808, doi: 10.1103/PhysRevLett.97.236808 (2006).
- [9] Diehl, S. et al. Quantum states and phases in driven open quantum systems with cold atoms. *Nature Phys.* **4**, 878 - 883, doi: 10.1038/nphys1073 (2008).
- [10] Verstraete, F., Wolf, M. M. & Cirac, J. I. Quantum computation and quantum-state engineering driven by dissipation. *Nature Phys.* **5**, 633 - 636, doi: 10.1038/nphys1342 (2009).
- [11] Fano, U. Effects of Configuration Interaction on Intensities and Phase Shifts. *Phys. Rev.* **124**, 1866-1878, doi: 10.1103/PhysRev.124.1866 (1961).
- [12] Anderson, P. W. Localized Magnetic States in Metals. *Phys. Rev.* **124**, 41-53, doi: 10.1103/PhysRev.124.41 (1961).
- [13] Cassettari, D., Hessmo, B., Folman, R., Maier, T. & Schmiedmayer, J. Beam Splitter for Guided Atoms. *Phys. Rev. Lett.* **85**, 5483-5487, doi: 10.1103/PhysRevLett.85.5483 (2000).
- [14] Leggett, A. J. *et al.* Dynamics of the dissipative two-state system. *Rev. Mod. Phys.* **59**, 1-85, doi: 10.1103/RevModPhys.59.1 (1987).

- [15] Yurke, B., McCall, S. L. & Klander, J. R. $SU(2)$ and $SU(1, 1)$ interferometers. *Phys. Rev. A* **33**, 4033-4054, doi: 10.1103/PhysRevA.33.4033 (1986).
- [16] Heidmann, A. *et al.* Observation of Quantum Noise Reduction on Twin Laser Beams. *Phys. Rev. Lett.* **59**, 2555-2557, doi: 10.1103/PhysRevLett.59.2555 (1987).
- [17] Braunstein, S. L. & Kimble, H. J. Teleportation of Continuous Quantum Variables. *Phys. Rev. Lett.* **80**, 869-872, doi: 10.1103/PhysRevLett.80.869 (1998).
- [18] Einstein, A., Podolsky, B. & Rosen, N. Can Quantum-Mechanical Description of Physical Reality Be Considered Complete? *Phys. Rev.* **47**, 777-780, doi: 10.1103/PhysRev.47.777 (1935).
- [19] Lidar, D. A., Chuang, I. L. & Whaley, K. B. Decoherence-Free Subspaces for Quantum Computation. *Phys. Rev. Lett.* **81**, 2594-2597, doi: 10.1103/PhysRevLett.81.2594 (1998).
- [20] Tan, H. T. & Zhang, W. M. Non-Markovian dynamics of an open quantum system with initial system-reservoir correlations: A nanocavity coupled to a coupled-resonator optical waveguide. *Phys. Rev. A* **83**, 032102, doi: 10.1103/PhysRevA.83.032102 (2011).
- [21] Schwinger, J. Brownian Motion of a Quantum Oscillator. *J. Math. Phys. (N.Y.)* **2**, 407-432, doi: 10.1063/1.1703727 (1961)
- [22] Keldysh, L.V. Diagram Technique for Nonequilibrium Processes. *Sov. Phys. JETP* **20**, 1018-1026 (1965).
- [23] Kadanoff, L. P. & Baym, G. *Quantum Statistical Mechanics* (Benjamin, New York, 1962).
- [24] Zhang, W. M., Lo, P. Y., Xiong, H. N., Tu, Matisse W. Y. & Nori, F. General Non-Markovian Dynamics of Open Quantum Systems. *Phys. Rev. Lett.* **109**, 170402, doi: 10.1103/PhysRevLett.109.170402 (2012).
- [25] Mahan, G. D. *Many-Body Physics*, 3rd Ed. (Kluwer Academic/Plenum Publishers, New Yoek, 2000).
- [26] Anderson, P. W. Absence of Diffusion in Certain Random Lattices. *Phys. Rev.* **109**, 1492-1505, doi: 10.1103/PhysRev.109.1492 (1958).
- [27] Cai, C. Y., Yang, L. P. & Sun, C. P. Threshold for nonthermal stabilization of open quantum systems. *Phys. Rev. A* **89**, 012128, doi: 10.1103/PhysRevA.89.012128 (2014).
- [28] Lo, P. Y., Xiong, H. N. & Zhang, W. M. Breakdown of Bose-Einstein Distribution in Photonic Crystals. *Sci. Rep.* **5**, 9423, doi: 10.1038/srep09423 (2015).
- [29] Nandkishore, R. & Huse, D. A. Many-Body Localization and Thermalization in Quantum

- Statistical Mechanics. *Ann. Rev. of Conden. Matter Phys.* **6**, 15-38, doi: 10.1146/annurev-conmatphys-031214-014726 (2015).
- [30] Xiong, H. N., Lo, P. Y., W. M. Zhang, Feng, D. H. & Nori, F. Non-Markovian Complexity in the Quantum-to-Classical Transition. *Sci. Rep.* **5**, 13353, doi: 10.1038/srep13353 (2015).
- [31] Vidal, G. & Werner, R. F. Computable measure of entanglement. *Phys. Rev. A* **65**, 032314, doi: 10.1103/PhysRevA.65.032314 (2002).
- [32] Simon, R. Peres-Horodecki Separability Criterion for Continuous Variable Systems. *Phys. Rev. Lett.* **84**, 2726-2729, doi: 10.1103/PhysRevLett.84.2726 (2000).
- [33] An, J. H. & Zhang, W. M. Non-Markovian entanglement dynamics of noisy continuous-variable quantum channels. *Phys. Rev. A* **76**, 042127, doi: 10.1103/PhysRevA.76.042127 (2007).
- [34] Paz, J. P. & Roncaglia, A. J. Dynamical phases for the evolution of the entanglement between two oscillators coupled to the same environment. *Phys. Rev. A* **79**, 032102, doi: 10.1103/PhysRevA.79.032102 (2009).

Acknowledgments.

We thank Dr. Ping-Yuan Lo for some useful discussions. This research is supported by the Ministry of Science and Technology of ROC under Contract No. NSC-102-2112-M-006-016-MY3. It is also supported in part by the Headquarters of University Advancement at the National Cheng Kung University, which is sponsored by the Ministry of Education of ROC.

Author Contributions

Y. C. L. and P. Y. Y. performed the theoretical calculations and prepared all the figures; W. M. Z. proposed the ideas and wrote the main manuscript. All authors participated the discussions and revised the manuscript.

Competing financial interests

The authors declare no competing financial interests.

Additional Information

Correspondence and requests for materials should be addressed to W. M. Zhang (wzhang@mail.ncku.edu.tw).